Electronic Supplementary Material (ESI) for Journal of Materials Chemistry A.

Supporting Information

Morphology, crystal structure and electronic state one-step co-tuning strategy towards developing superior perovskite electrocatalyst for water oxidation

Haijuan Zhang,[a] Daqin Guan,[a] Xuechao Gao,[a] Gao Chen,[a] Jie Yu,[a] Wei Zhou,[a*] Zongping Shao[a,b*]

[a] *State Key Laboratory of Materials-Oriented Chemical Engineering, College of Chemical Engineering, Nanjing Tech University, Nanjing, 210009, PR China.*

[b] *Department of Chemical Engineering, Curtin University, Perth, Western Australia, 6845, Australia.*

Catalyst synthesis.

Synthesis of the bulk SBSC catalysts at different temperatures. The bulk SBSC catalysts were prepared by a combined ethylenediaminetetraacetic acid (EDTA)-citrate (CA) complexing sol-gel method. In short, $Sm(NO_3)_3$, $Ba(NO_3)_2$, $Sr(NO_3)_2$ and $Co(NO_3)_2 \cdot 6H_2O$ (all of analytical grade, Sinopharm Chemical Reagent Co., Ltd.)were dissolved in deionized water, followed by a mixed solution of EDTA ($C_{10}H_{16}N_2O_8$, Sinopharm Chemical Reagent Co., Ltd.) and CA ($C_6H_8O_7$, Sinopharm Chemical Reagent Co., Ltd.) at a molar ratio of 1:1:2 for total metal ions:EDTA:citric acid. Then, an aqueous ammonium hydroxide solution (NH_3, 28%, Sinopharm Chemical Reagent Co., Ltd.) was added to adjust the solution pH value to ≈6. Afterwards, the solution was continuously stirred at 90 °C to yield a gel, and the resulting gel was held at 250 °C to form a solid precursor. The precursors were respective calcined at 950, 1000, 1050 and 1100 °C and labeled SBSC-S(950), SBSC-S(1000), SBSC-S(1050) and SBSC-S(1100), respectively. In addition, iridium oxide (IrO_2, 99.9%, metals basis) were obtained from Aladdin Industrial Corporation (Shanghai, China).

Synthesis of SBSC nanofibers. SBSC nanofibers were synthesized via electrospinning followed by heating treatment to remove the organic precursor materials. In a typical procedure for electrospinning, $Sm(NO_3)_3$, $Ba(NO_3)_2$, $Sr(NO_3)_2$ and $Co(NO_3)_2 \cdot 6H_2O$, with a total amount of 2 mmol were dissolved in 10 mL of N,N-dimethylformamide(DMF, Sinopharm Chemical Reagent Co., Ltd.) at room temperature. Then, 1 g of polyvinylpyrrolidone (PVP, Mv.1300000, Sinopharm Chemical Reagent Co., Ltd.) was added, and the resulting solution was stirred overnight to ensure that the PVP was fully dissolved. The as-prepared SBSC precursor solution was added to a plastic syringe equipped with a 23-gauge needle for electrospinning. The distance between the needle tip and the collector was approximately 15 cm, and the applied voltage was fixed at 18 kV. The nanofibers were deposited onto aluminum foil at a feeding rate of 1.5 ml h^{-1}. The as-spun nanofibers were calcined at 800, 950 and 1100 °C. The obtained products were labelled SBSC-E(800), SBSC-E(950) and SBSC-E(1100), respectively.

Material characterization.

The phase structures were characterized by X-ray powder diffraction (XRD, Rigaku Smartlab 3kW) with filtered Cu Kα radiation (λ = 1.5406 Å, 40 kV, 40 mA) in the 2θ range of 20°–90° at an interval of 0.02°. The microstructures and morphologies of the catalysts were analysed by scanning electron

microscopy (SEM, S-4800) and transmission electron microscopy (TEM, JEM-2100). EDS elemental mapping was performed on an FEI Tecnai G2 F30 STWIN field-emission transmission electron microscope equipped with an EDX analyser and operated at 200 kV. The specific surface areas and the corresponding pore size distributions were characterized by nitrogen adsorption tests (BELSORP II) using the Brunauer-Emmett-Teller (BET) and Barrett–Joyner–Halenda (BTH) methods. Thermal gravimetric (TG)-differential thermal analysis (DTA) curves and ion currents for CO_2 plots in air were obtained in a TG-MS (NETZSCHSTA339F3-QMS403D). The surface elemental states were determined by X-ray photoelectron spectroscopy (XPS, PHI5000 VersaProbe) equipped with an Al Kα X-ray source. The soft X-ray absorption spectroscopy (XAS) spectra were tested at the BL11A beamline.

Electrochemical measurement of the OER activities

Working Electrode Preparation. The working electrodes were prepared by a controlled drop-casting method involving a rotating disk electrode (RDE) made of glassy carbon (GC, 0.196 cm^2, Pine Research Instrumentation). The GC electrodes were polished with α-Al_2O_3 slurries and rinsed with ethanol before use. The catalyst ink was prepared by sonicating a mixture of 10.0 mg of catalyst, 10.0 mg of conductive carbon (Super P Li) and 100.0 μL of a 5 wt% Nafion solution dispersed in 1.0 mL of absolute ethanol for approximately 1 h to generate a homogeneous ink. Then, 5 μL of the catalyst ink was transferred onto the surface of the GC substrate, yielding an approximate catalyst loading of 0.232 mg_{oxided} cm^{-2}. The same mass loading was used for all the catalysts and commercial IrO_2 for all the electrochemical measurements.

Electrochemical Measurements. Electrochemical measurements were performed with a standard three-electrode electrochemical cell (Pine Research Instrumentation) with an RDE configuration controlled by a CHI 760D electrochemistry workstation in a 0.1 M KOH aqueous solution at room temperature. Ag/AgCl and Pt were used as the reference and counter electrodes, respectively. The electrolyte was bubbled with oxygen to ensure O_2-saturation during the test period and ensure the O_2/H_2O equilibrium at 1.23 V versus RHE. The OER polarization curves obtained from LSV were recorded at a scan rate of 5 mV s^{-1} from 0.2 to 1.0 V versus Ag/AgCl with a rotation rate of 1,600 r.p.m. Electrochemical impedance spectroscopy (EIS) was performed from 100 kHz to 0.1 Hz at 0.7 V versus Ag/AgCl under the influence of an AC voltage of 10 mV. CV tests were used to measure

the electrochemical double layer capacitance (Cdl). The potential was swept from −0.8 to −0.9 V versus Ag/AgCl at different scan rates of 20, 30, 40, 60, 80 and 100 mV s^{-1}.

Theoretical calculation

DFT computations were performed with the material studio using the castep calculation method. The General Gradient Approximation with the Perdew Burke Ernzenhof functional was applied and kinetic energy cutoff was 330 eV. $SmBa_{0.5}Sr_{0.5}Co_2O_{6-\delta}$ perovskites with cubic and tetragonal structure were simulated based on the reported structures within the 2 × 2 × 2 perovskite cell and sampled by a 1 × 1 × 1 Monkhorst-Pack k-point mesh. An effective O p-band center was determined by taking the centroid of the projected density of states of O 2p states relative to the Fermi level.

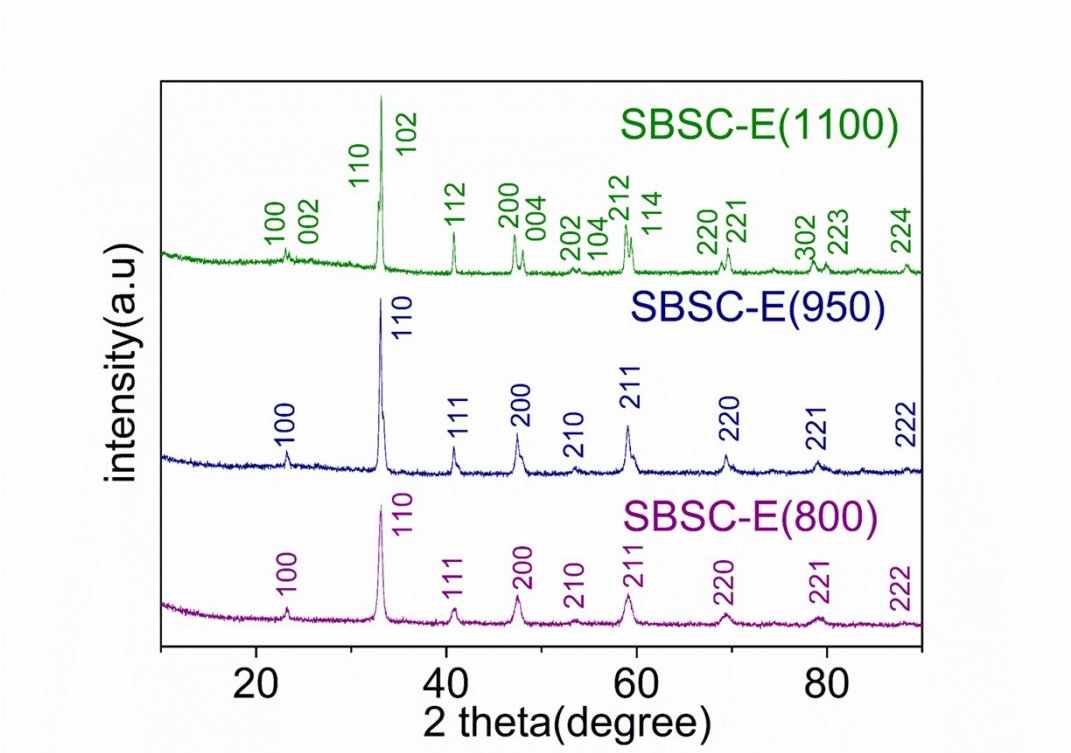

Figure S1. XRD patterns of SBSC-E(800), SBSC-E(950) and SBSC-E(1100).

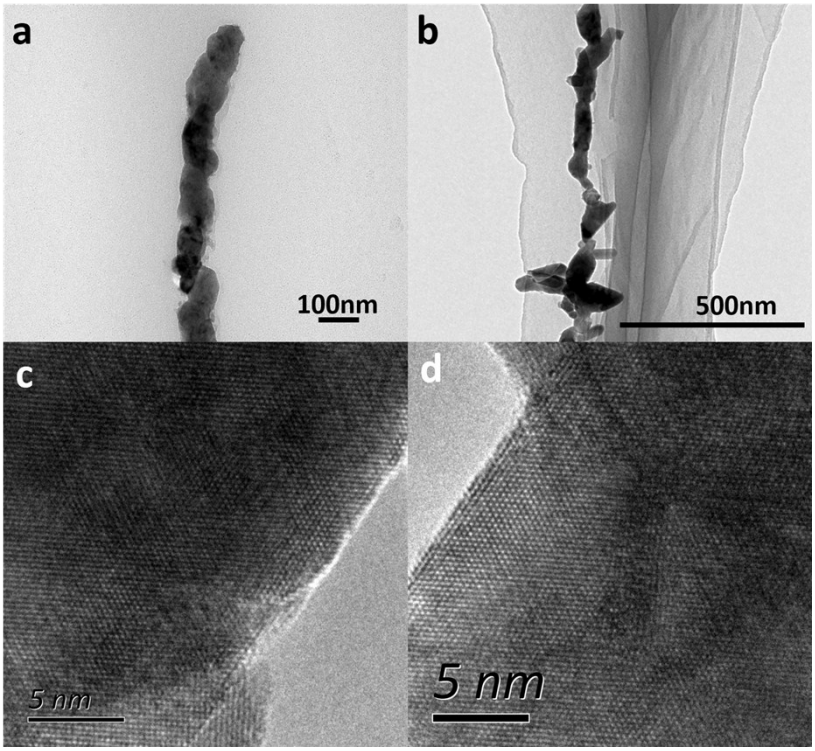

Figure S2. HRTEM images of SBSC-E(800).

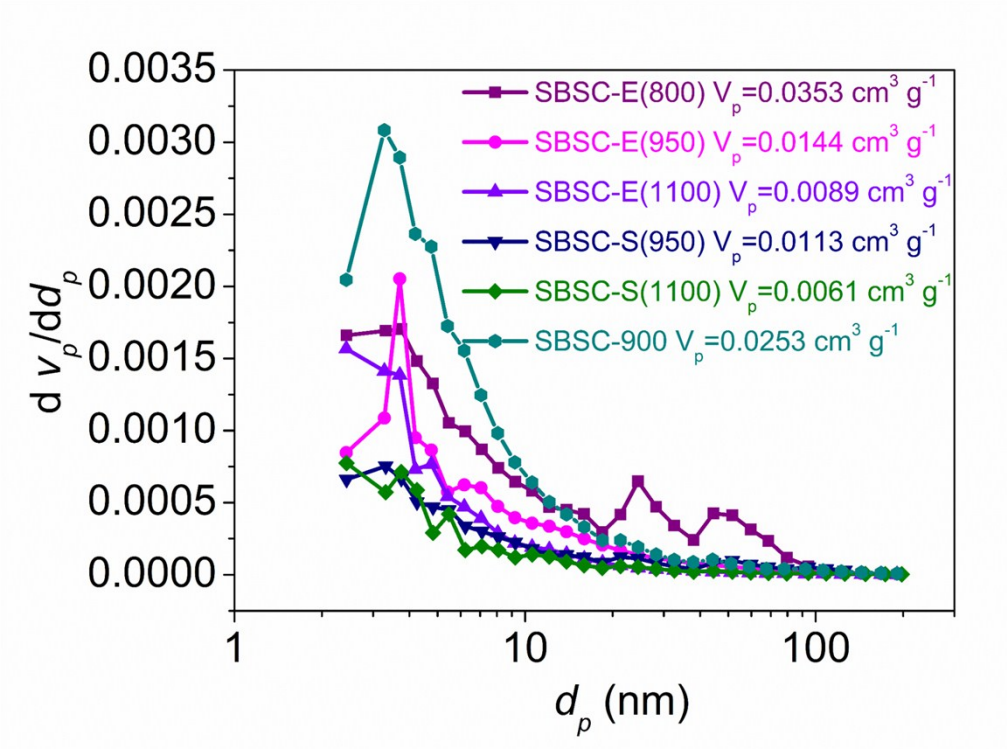

Figure S3. Corresponding Barrett-Joyner-Halenda (BJH) pore size distribution plots of all samples.

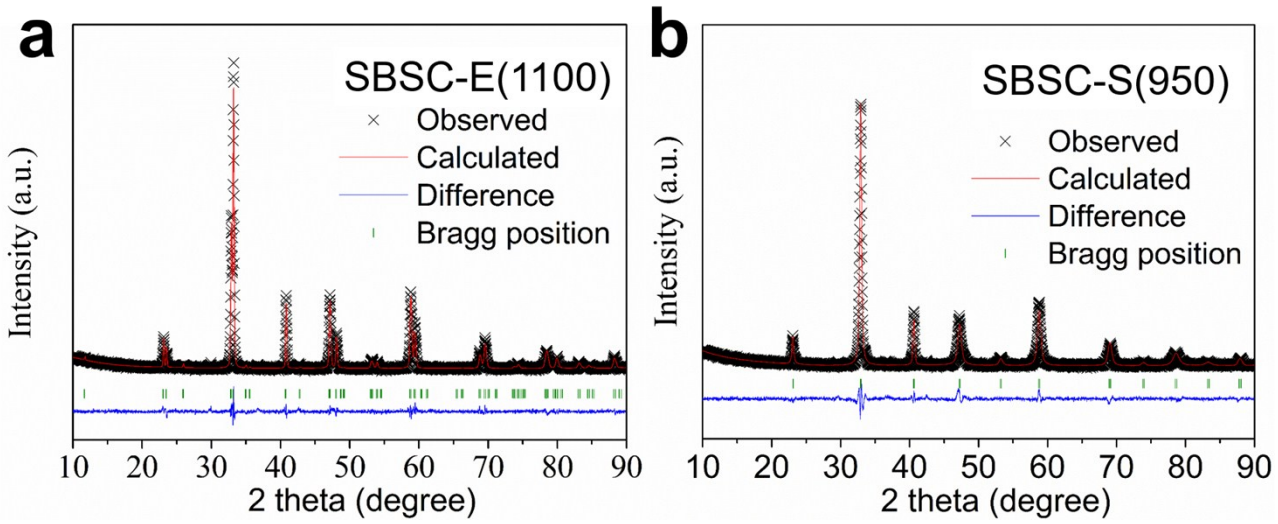

Figure S4. Rietveld refinement XRD patterns of (a) SBSC-E(1100) and (b) SBSC-S(950).

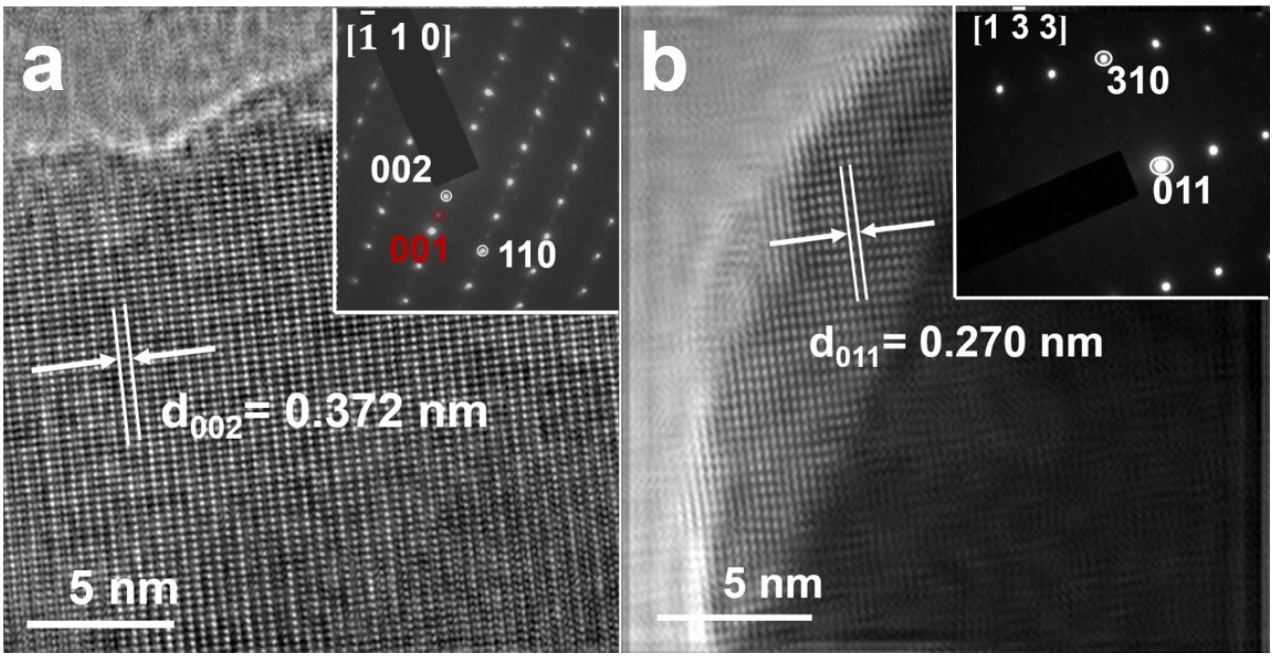

Figure S5. HRTEM image of (a) SBSC-E(1100) and (b) SBSC-S(950).

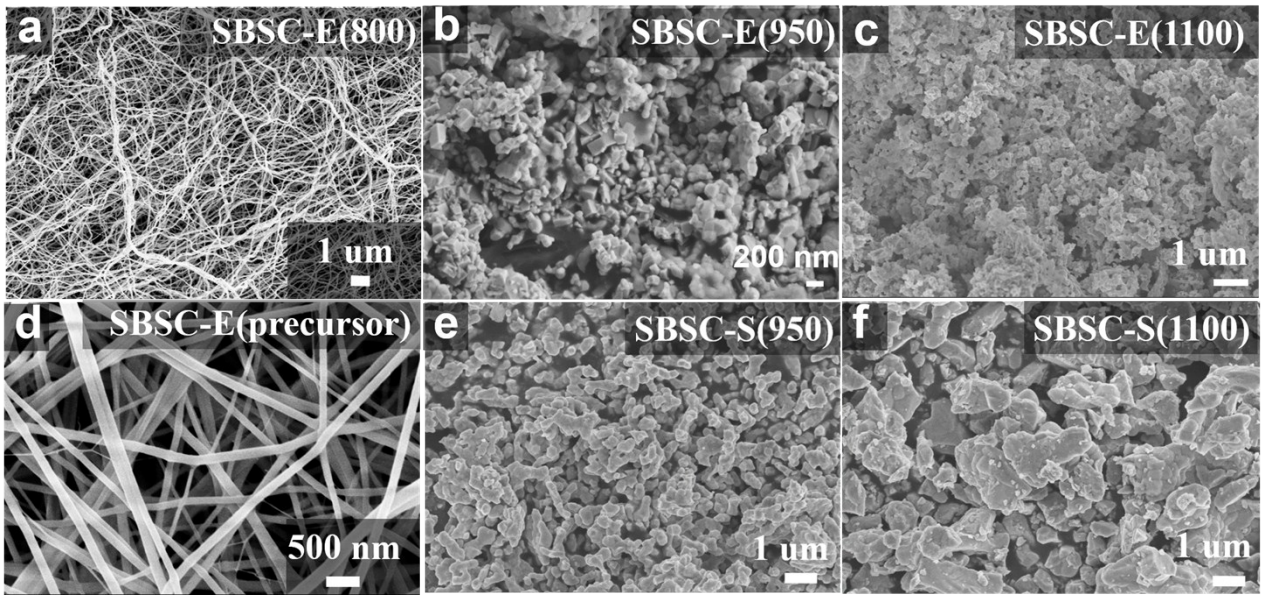

Figure S6. SEM images of samples. (a) SBSC-E(800); (b) SBSC-E(950); (c) SBSC-E(1100); (d) SBSC-E(precursor); (e) SBSC-S(950); (f) SBSC-S(1100).

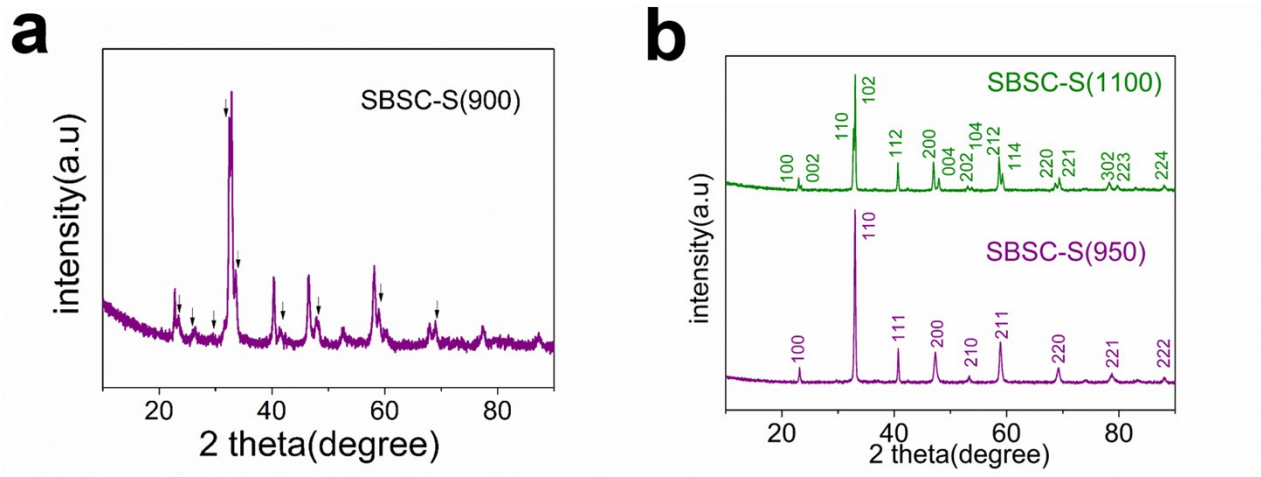

Figure S7. XRD patterns of SBSC-S(900), SBSC-S950) and SBSC-S(1100).

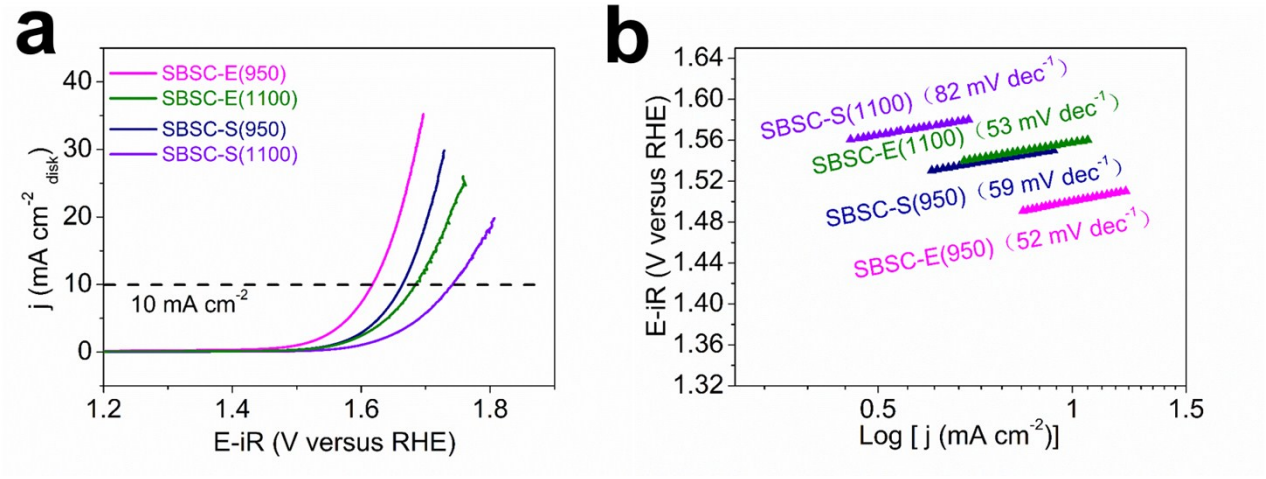

Figure S8. (a) The iR-corrected linear sweep voltammetry (LSV) OER polarization curves and (b) the corresponding Tafel plots of SBSC-E(950), SBSC-E(1100), SBSC-S(950) and SBSC-S(1100) catalysts loaded onto a RDE (1600 rpm) in an O_2-saturated 0.1 M KOH solution.

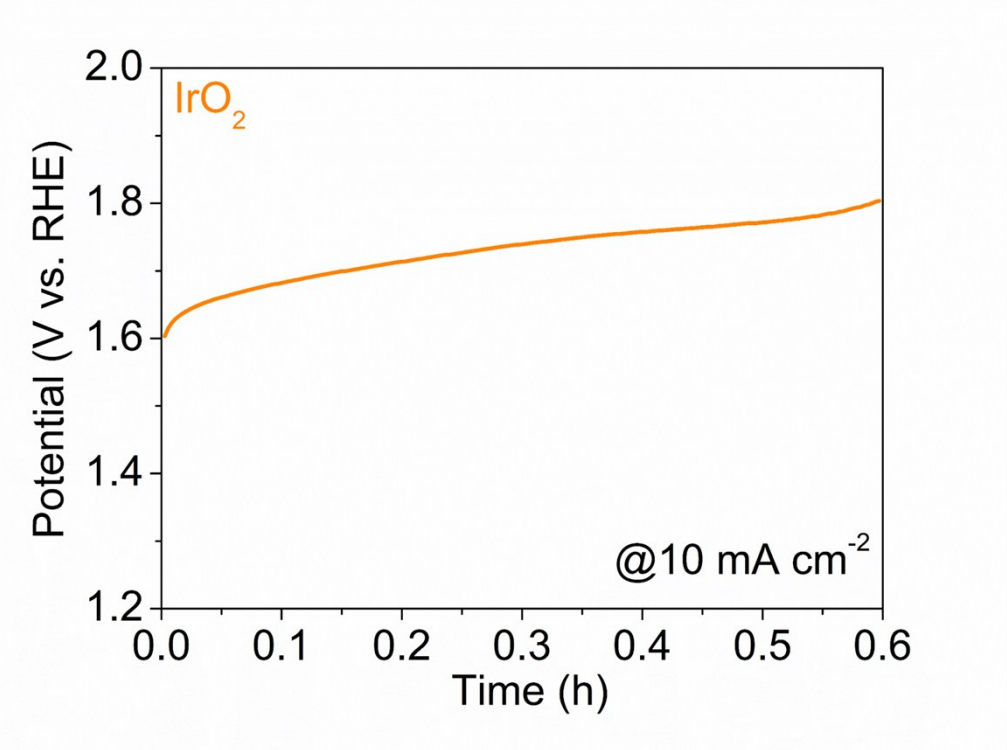

Figure S9. Chronopotentiometric curves of IrO_2 at 10 mA cm^{-2}.

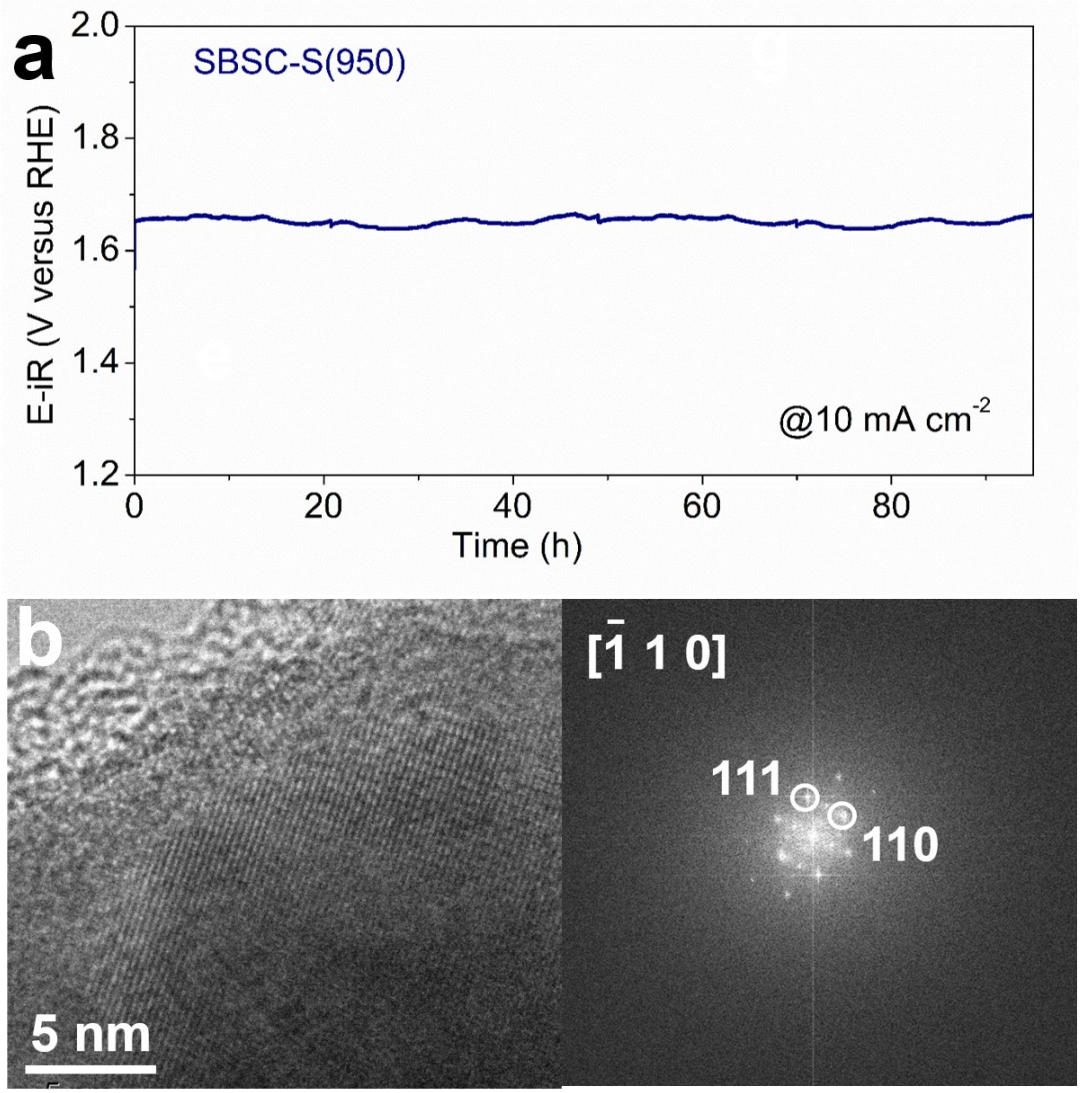

Figure S10. (a) Chronopotentiometric curves of SBSC-S(950) at 10 mA cm^{-2}. (b) HRTEM images and fast Fourier transforms (FFTs) pattern of SBSC-S(950) samples after measuring the chronopotentiometric curves.

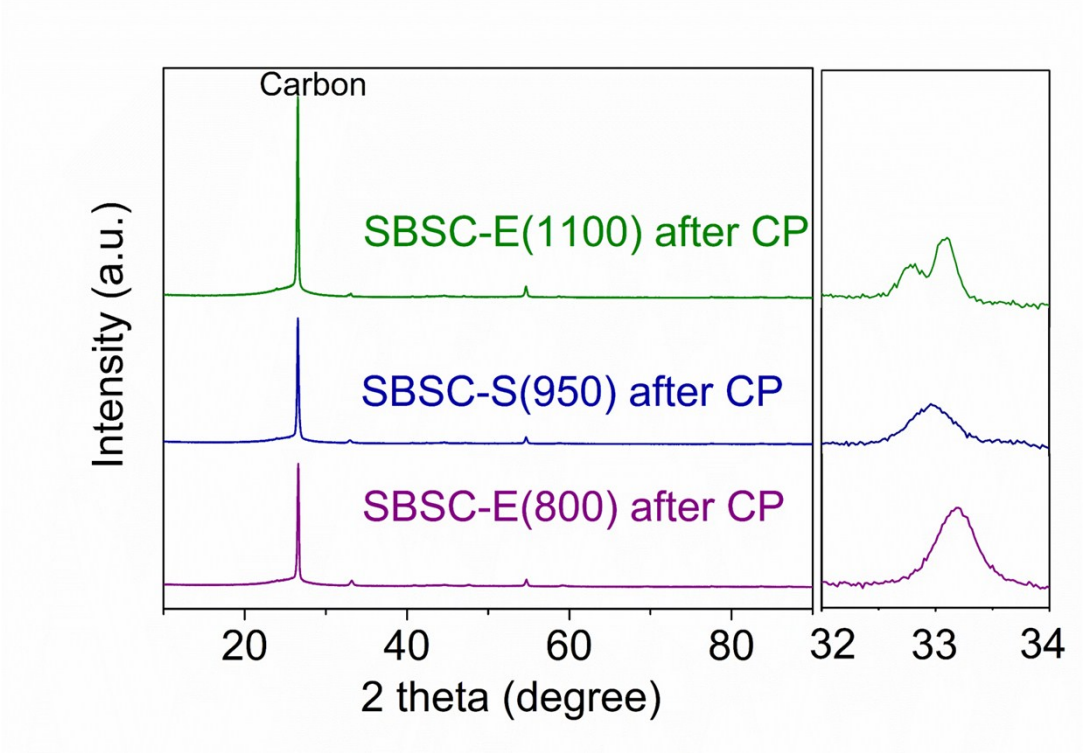

Figure S11. XRD patterns of SBSC-E(800), SBSC-E(1100) and SBSC-S(950) after Chronopotentiometric curves.

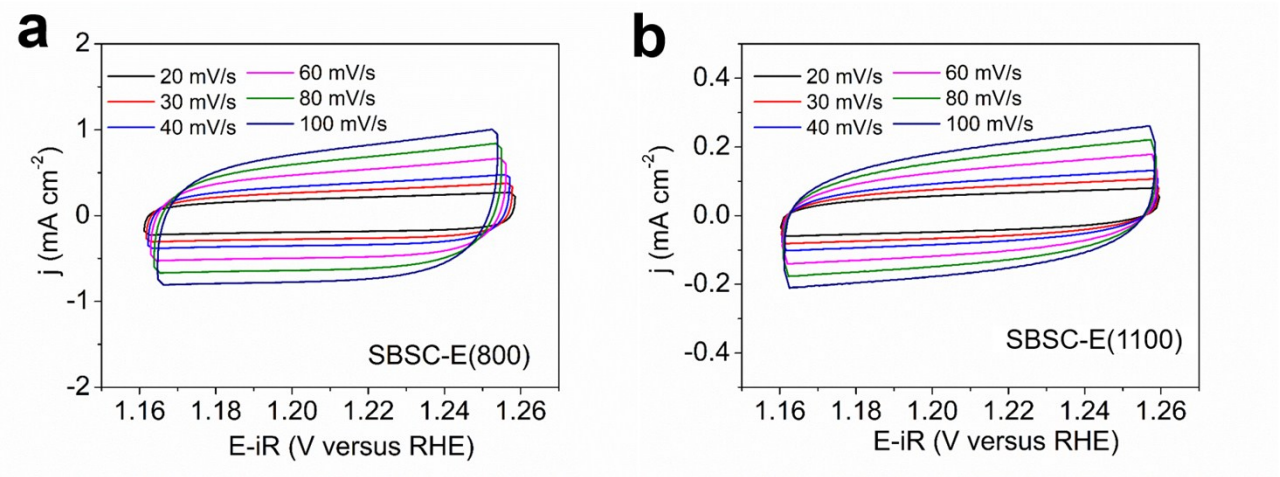

Figure S12. Electrochemical CV scans (1.16-1.26 V vs. RHE) recorded for (a) SBSC-E(800), and (b) SBSC-E(1100) at different potential scanning rates. Scan rates are 20, 30, 40, 60, 80 and 100 mV s^{-1}.

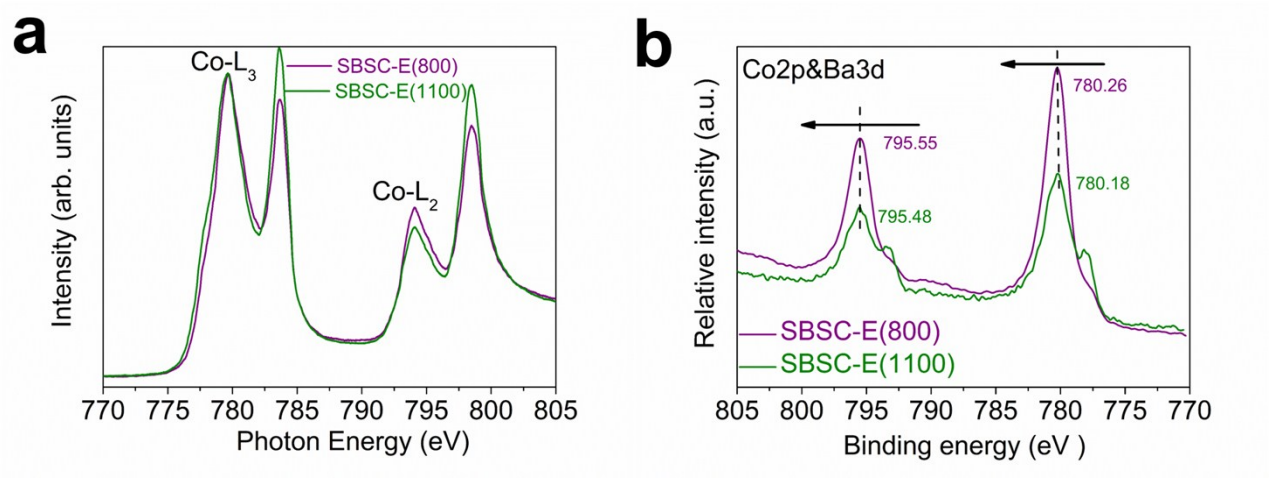

Figure S13. SBSC-E(800) and SBSC-E(1100) catalysts (a) Co-$L_{2,3}$ XAS spectra (b) Co2p/Ba3d XPS spectra.

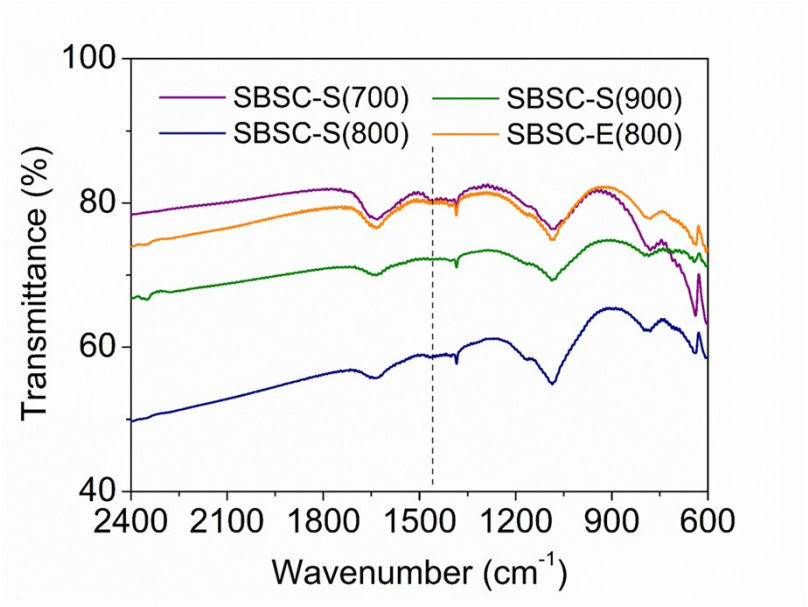

Figure S14. FTIR spectra of SBSC-S(700), SBSC-S(800), SBSC-S(900) and SBSC-E(800).

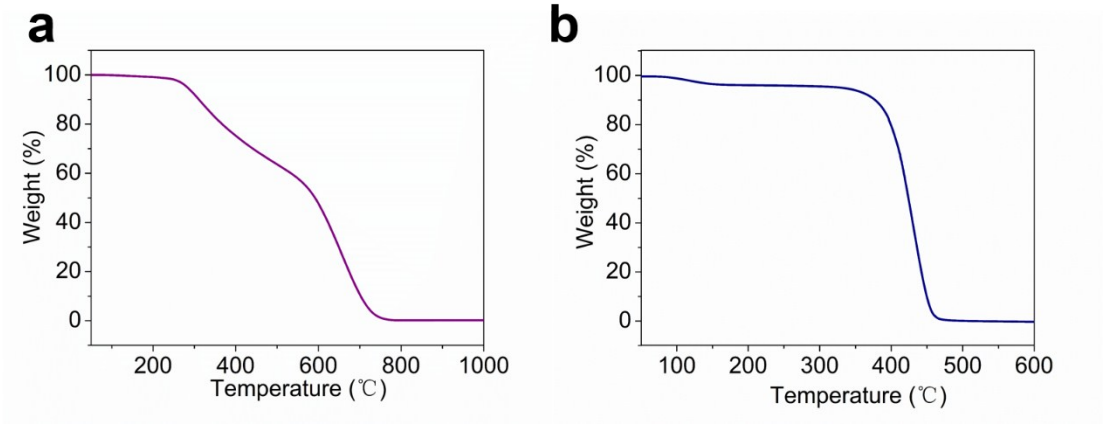

Figure S15. TG plot of samples by (a) sol-gel and (b) electrospinning without metal salt.

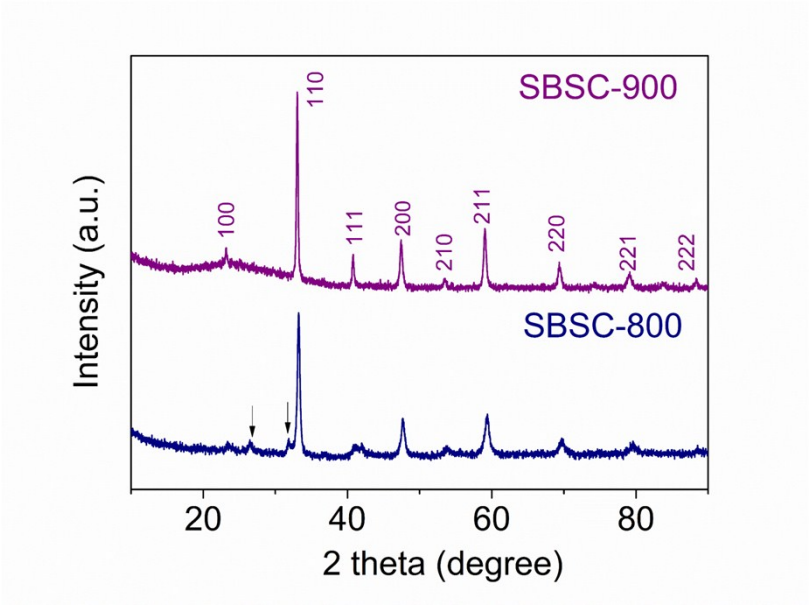

Figure S16. XRD patterns of SBSC by calcining the electrospinning solution directly.

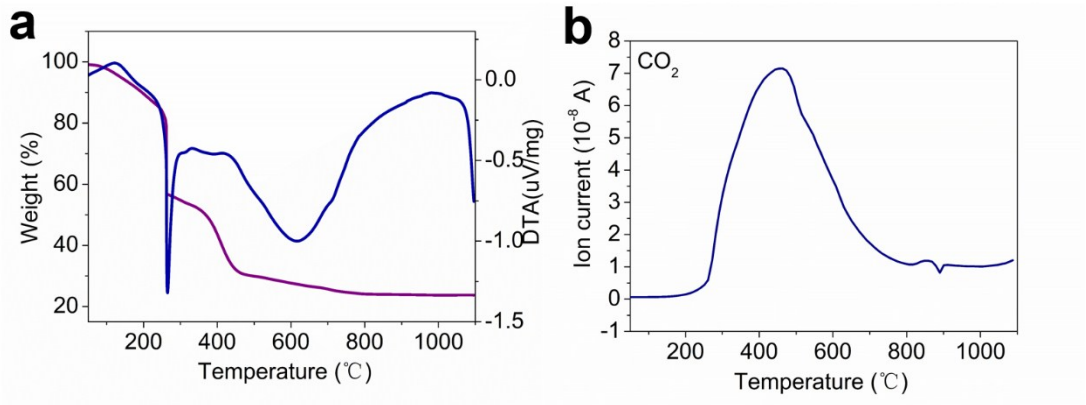

Figure S17. (a) TG-DSC plot and (b) Ion currents with CO_2 of SBSC solution of electrospinning.

Table S1 Rietveld refined lattice parameters and reliability factors for perovskites

Perovskites	Space group	Lattice parameter (Å)	χ^2	R_p (%)	R_{wp} (%)
SBSC-E(800)	*P*mm	a=3.8313	1.087	4.21	5.32
SBSC-E(1100)	*P*4/mmm	a=b=3.8610, c=7.5810	1.466	3.04	3.90
SBSC-S(950)	*P*mm	a=3.8486	1.820	3.19	4.17

Table S2 BET specific surface areas of the catalysts.

Perovskites	Specific surface area / m^2 g^{-1}
SBSC-E(800)	13.1
SBSC-E(950)	5.2
SBSC-E(1100)	4.9
SBSC-S(950)	4.5
SBSC-S(1100)	3.1
SBSC-900	10.8
IrO_2	146.9

Table S3 Comparison of OER performance of our catalysts with reported representative active OER electrocatalysts

Perovskites	Electrolyte	η@10 mA cm^{-2} (mV)	Tafel slope (mV dec^{-1})	Reference
SBSC-E(800)	0.1 M KOH	370	46	This work
PBSCF-20nm	0.1 M KOH	358	52	*Nat. Commun.* **2017**, 8, 14586
SNCF-NRs	0.1 M KOH	390	61	*Adv. Energy Mater.* **2017**, 7, 1602122

L0.5BSCCF/rGO	1 M KOH	338	80	*Adv. Energy Mater.* **2017**, 7, 1700666
SSC-HG	0.1 M KOH	400	115	*Small.* **2018**, 1802767
$LaSr_3Co_{1.5}Fe_{1.5}O_{10-\delta}$	0.1 M KOH	388	83.9	*Nano Energy.* **2017**, 40, 2211
$NdBaMn_2O_{5.5}$	0.1 M KOH	400	75	*ACS Catal.* **2018**, 8, 364
LCO-80 nm	0.1 M KOH	490	69	*Nat. Commun.* **2016**, 7, 11510
SCFW0.4-BM	0.1 M KOH	357	58	*J. Mater. Chem. A.* **2018**, 6, 9854
SCP	0.1 M KOH	480	84	*Adv. Funct. Mater.* **2016**, 26, 5862
NBSC-pPy	0.1 M KOH	420	n.a.	Energy Environ. Sci. **2017,**10, 523
IrO_2	0.1 M KOH	372	58	This work

Table S4 Mass activities and BET surface area-normalized intrinsic activities of catalysts at η=0.37

Perovskites	Mass activity (A g^{-1}_{oxide})	Intrinsic (specific) activity (A m^{-2}_{oxide})
SBSC-E(800)	43.1	3.3
SBSC-E(950)	31.5	6.1
SBSC-E(1100)	10.2	2.1
SBSC-S(950)	12.2	2.7
SBSC-S(1100)	3.9	1.2
SBSC-900	24.1	2.2
IrO_2	40.8	0.3

Table S5 The relative amounts of the four different surface oxygen species of SBSC

Perovskite	H_2O (%)	-OH/O_2 (%)	O^{2-}/O^{-} (%)	O^{2-} (%)
SBSC-E(800)	12.27 %	59.69 %	19.38 %	8.66 %
SBSC-E(1100)	11.68 %	50.94 %	19.29 %	18.09 %